

**Inverted hysteresis and negative remanence in a homogeneous antiferromagnet**L. Opherden,<sup>1,2,\*</sup> T. Bilitewski,<sup>3</sup> J. Hornung,<sup>1,2</sup> T. Herrmannsdörfer,<sup>1</sup> A. Samartzis,<sup>4,5</sup> A. T. M. N. Islam,<sup>4</sup> V. K. Anand,<sup>4</sup> B. Lake,<sup>4,5</sup> R. Moessner,<sup>3</sup> and J. Wosnitza<sup>1,2</sup><sup>1</sup>Hochfeld-Magnetlabor Dresden (HLD-EMFL), Helmholtz-Zentrum Dresden-Rossendorf, 01328 Dresden, Germany<sup>2</sup>Institut für Festkörper- und Materialphysik, TU Dresden, 01062 Dresden, Germany<sup>3</sup>Max-Planck-Institut für Physik komplexer Systeme, 01187 Dresden, Germany<sup>4</sup>Helmholtz-Zentrum Berlin für Materialien und Energie GmbH, Hahn-Meitner Platz 1, 14109 Berlin, Germany<sup>5</sup>Institut für Festkörperphysik, Technische Universität Berlin, Hardenbergstraße 36, 10623 Berlin, Germany

(Received 15 May 2018; published 7 November 2018)

Magnetic remanence—found in bar magnets or magnetic storage devices—is probably the oldest and most ubiquitous phenomenon underpinning the technological applications of magnetism. It is a macroscopic nonequilibrium phenomenon: A remanent magnetization appears when a magnetic field is applied to an initially unmagnetized ferromagnet, and then taken away. Here, we present an inverted magnetic hysteresis loop in the pyrochlore compound  $\text{Nd}_2\text{Hf}_2\text{O}_7$ : The remanent magnetization points in a direction *opposite* to the applied field. This phenomenon is exquisitely tunable as a function of the protocol in field and temperature, and it is reproducible as in a quasiequilibrium setting.

DOI: [10.1103/PhysRevB.98.180403](https://doi.org/10.1103/PhysRevB.98.180403)

The “all-in–all-out” state of pyrochlore magnets plays an important role in the study of topological magnets on account of its role in the genesis of condensed-matter axion electrodynamics [1–4]. Here, we study its response to an applied field in the insulating magnetic pyrochlore compound  $\text{Nd}_2\text{Hf}_2\text{O}_7$ . We report the observation of a fully inverted magnetic hysteresis loop probed by the dynamic susceptibility resulting in a negative remanence in the low-field part of the all-in–all-out ordered phase. We propose an effective theory for this phenomenon in terms of the nonequilibrium population of domain walls which exhibit a magnetic moment between domains of an ordered antiferromagnetic state which itself has zero net magnetization.

$\text{Nd}_2\text{Hf}_2\text{O}_7$  belongs to the class of cubic pyrochlore oxides [5] of the composition  $R_2T_2O_7$ , where  $R$  is typically a trivalent rare-earth ion and  $T$  a tetravalent transition-metal ion. In these structures the  $R$  and the  $T$  ions both form a sublattice of corner-sharing tetrahedra (Fig. 1). An asymmetrical arrangement of eight bivalent oxygen ions around each  $R$  ion leads to a strong crystal electric field (CEF) splitting of their  $J + 1$  multiplet by several hundred degrees Kelvin [5]. The resulting CEF ground state is a pseudospin-half state with a strong local anisotropy and the spins are forced to point along the corner-to-center direction of each tetrahedron corresponding to the four equivalent local  $\langle 111 \rangle$  directions of the cubic lattice. In the all-in–all-out state all spins in a tetrahedron either point in or out, resulting in two distinct realizations: A fourth of the spins are oriented either parallel (AIAO) or antiparallel (AOAI) to the  $[111]$  axis. This allows for the formation of domains which are sensitive to an applied magnetic field along the  $[111]$  direction, as shown for several all-in–all-out ordered pyrochlores [6–11].

The antiferromagnetic all-in–all-out-order is realized in several pyrochlores, such as iridium-based compounds  $R_2\text{Ir}_2\text{O}_7$  ( $R = \text{Y, Nd, Sm, Eu, Tb}$ ) [12–16] or  $\text{Cd}_2\text{Os}_2\text{O}_7$  [17] where usually both sublattices adopt this order accompanied by a metal-insulator transition. In the case of nonmagnetic  $T$  ions, all-in–all-out ordering was found in the insulating neodymium-based compounds  $\text{Nd}_2\text{Sn}_2\text{O}_7$  [18],  $\text{Nd}_2\text{Zr}_2\text{O}_7$  [19,20], and  $\text{Nd}_2\text{Hf}_2\text{O}_7$  [21] with a Néel temperature below 1 K.

The formation of antiferromagnetic domains was observed for several of these systems [7,9–11,22,23], and inverted hysteresis of the magnetization has been reported for  $\text{Nd}_2\text{Ir}_2\text{O}_7$  [13,24] and  $\text{Nd}_2\text{Zr}_2\text{O}_7$  [25]. However,  $\text{Nd}_2\text{Hf}_2\text{O}_7$  is the first all-in–all-out antiferromagnet where a negative remanent magnetization has been observed.

The underlying all-in–all-out order in  $\text{Nd}_2\text{Hf}_2\text{O}_7$  is established below  $T_N = 0.48$  K and is stable for external magnetic fields up to  $\mu_0 H_{\text{dc}} = 0.27$  T (Fig. 3 and Fig. S2 [26]).

The hysteresis behavior shows the following salient properties: There is (a) an inverted hysteresis loop with a large negative remanent magnetization, (b) which is stable, reproducible, and fully tunable by cooling the sample in a finite field, and (c) can be reset by applying a heat pulse above  $T_N$ ; finally, (d) is highly anisotropic, only occurring for specific field directions.

The fully inverted hysteresis loop of  $\text{Nd}_2\text{Hf}_2\text{O}_7$  observed for  $H \parallel [111]$  (Fig. 2) covers a fixed area between a temperature-dependent value of  $\pm H^*(T)$  (up to 0.14 T at 0.12 K for  $H \parallel [111]$ ) where the susceptibility shows a sharp and pronounced jump [Fig. 2(b)]. The hysteresis appears exclusively if the maximum applied field exceeds  $H^*$ , otherwise the behavior is free of hysteresis.  $H^*$  shows a strong temperature dependence for  $T \leq T_N$  (Fig. S3), and is significantly smaller than the critical field  $H_c$  at which the transition occurs for  $H \parallel [001]$  [Fig. S2(c)]. The hysteresis is absent for

\*l.opherden@hzdr.de

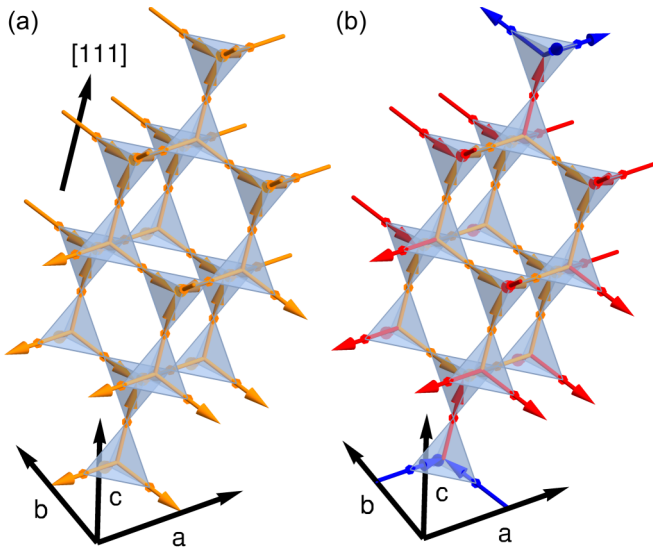


FIG. 1. Pyrochlore structure formed by a lattice of corner-sharing tetrahedra and all-in-all-out magnetic order. (a) All-in-all-out ordered state in the pyrochlore structure with  $a$ ,  $b$ ,  $c$  crystal axes and  $[111]$  direction indicated. All spins are oriented along their local  $(111)$  direction pointing either into or out from the center of their tetrahedra. Shown is the AIAO state, and the AOAI state (not shown) is obtained by flipping all spins. (b) Spherical AIAO domain in AOAI background oriented along  $[111]$  resulting in a negative magnetization. Blue (orange) spins belong to AOAI (AIAO) bulk tetrahedra, and red spins are boundary spins of the AIAO domain.

fields oriented along the  $[001]$  direction [Fig. S2(b)], and at temperatures larger than  $T_N$ .

We find a large coercivity, about 24 mT at a temperature of 0.12 K, to be compared to recent findings in ferromagnetic thin films which show a reversed hysteresis with a coercive field of only about 2 mT [27]. Also the remanence is unusually large at  $0.06\mu_B/\text{Nd}^{3+}$  (2.4% of the effective moment), several times larger than (the conventional “noninverted” hysteresis) in  $\text{Cd}_2\text{Os}_2\text{O}_7$  (up to  $6 \times 10^{-5}\mu_B/\text{Os}$ ) [23]. Other all-in-all-out ordered pyrochlores, such as  $\text{Nd}_2\text{Ir}_2\text{O}_7$  or  $\text{Nd}_2\text{Zr}_2\text{O}_7$ , show a similar inverted hysteresis loop of the susceptibility for  $H \parallel [111]$ , but with vanishing remanent magnetization [24,25,28].

Next, we demonstrate that the sample adopts distinct stable states depending on the field/temperature history. For each state, the observed hysteresis curves are robust to magnetic-field changes. In Figs. 2(c) and 2(e) we show that when staying below  $H^*$  the magnetization is free of hysteresis and the state is perfectly stable. The susceptibility follows a unique perfectly reproducible trajectory when sweeping the magnetic field back and forth staying below  $H^*$ , both when in the polarized state [Fig. 2(c), green data points] as well as in the unpolarized state [Fig. 2(e), violet data].

Moreover, one can reliably switch between the different states of the system. In Figs. 2(d) and 2(e), we show such a protocol. Starting in the positive polarized or unpolarized state sweeping the field below  $-H^*$  switches the system to the negative polarized state in which the susceptibility follows a distinct trajectory. Then, applying a thermal cycle above the

critical temperature after switching off the field allows one to return the sample to the unpolarized state.

Additionally, the observed hysteresis in the susceptibility may be continuously and fully tuned. By cooling the sample below  $T_N$  in a finite magnetic field  $|H^0| < |H^*|$ , we prepare a family of distinct states with associated susceptibility curves [Fig. 2(f)]. The observed trajectories continuously interpolate between the maximally polarized conditions. These states are again perfectly stable to changes in the magnetic field below the critical field with a unique trajectory defined by the initially prepared state. This is in stark contrast to the known behavior of ferromagnetic materials where a field change or temperature variation within the ordered state leads to domain-wall orientation, hence, a reduced hysteresis loop and different trajectories of  $m(H, T)$ .

Finally, we demonstrate that the AIAO ordered state of  $\text{Nd}_2\text{Hf}_2\text{O}_7$  splits into two phases as seen in the ac susceptibility for external magnetic fields applied along  $[111]$  (Fig. 3) as well as  $[110]$  (Fig. S5). At low fields and temperatures the system can adopt different states whereas at high fields a unique state appears.

For each field, the sample was cooled under an overcritical positive field (+), an overcritical negative field (−), and in zero field (0). At low temperatures the susceptibility of these states differs: The negatively polarized state shows a lower susceptibility than the positively polarized state with the unpolarized (zero-field-cooled) state intermediate between them.

For a sufficiently strong field we find a new phase setting in at larger temperatures where the susceptibility of the differently prepared states coincides. The entrance into this unique state is accompanied by a sharp change of  $\chi'$  for the negatively and nonpolarized states and the susceptibility only depends weakly on temperature within this phase. The temperature range where this state exists increases at increasing external field (blue shaded areas in Fig. 3 and Fig. S5). At an even higher temperature,  $\chi'(T)$  exhibits a peak (kink for higher fields) when the antiferromagnetic order is broken.

We construct the field-temperature phase diagram for  $H \parallel [111]$  [Fig. 3(b)] by the temperature of the kink as well as by the endpoints of the hysteresis in the temperature and field dependence of the ac susceptibility (Fig. 3 and Fig. S3). Whereas the kink represents the phase boundary to the all-in-all-out ordered state, the latter criteria separates the mixed domain state from the polarized domain state. The Supplemental Material [26] contains the corresponding phase diagrams for different field directions.

We interpret these results as originating from domains of the two possible realizations of the all-in-all-out order. At strong fields only the fully polarized domain state exists, whereas within the hysteretic part of the all-in-all-out state, the sample can contain any mixture of AIAO and AOAI domains. Preparing the sample in a finite field allows for tuning the ratio of AIAO to AOAI domains up to the fully polarized single domain state. The results then suggest that within each phase these domain configurations are stable to changes in temperature and magnetic field.

We propose an explanation of the anisotropic and inverted hysteresis and the negative remanent magnetization via the preferential formation of oppositely (to the magnetic field)

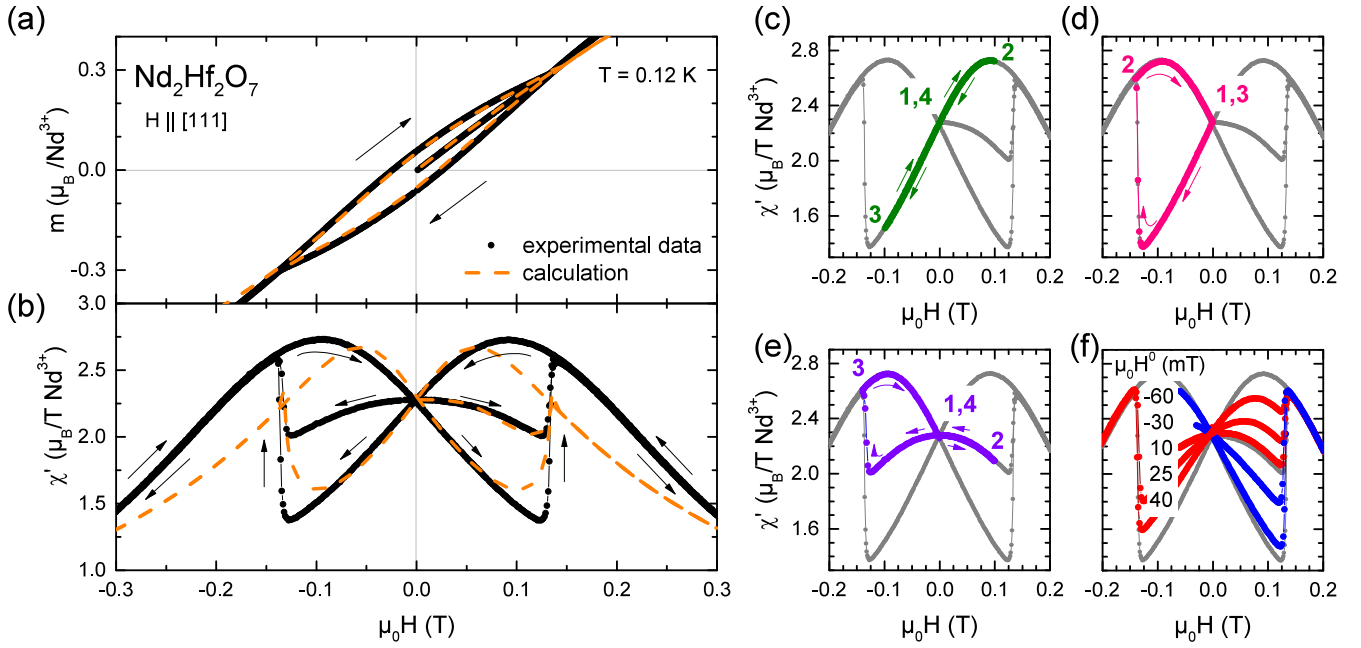


FIG. 2. Magnetic-field dependence of the dynamic susceptibility. (a,b) Experimental results (black line) and results from calculation (orange dashed line) of the magnetization (a) obtained by integrating the dynamic susceptibility (b), both for  $H \parallel [111]$  at a temperature of 0.12 K. For fields smaller than  $\pm 125$  mT ( $\pm H^*$ ) the susceptibility shows an inverted hysteresis. For higher fields a sharp transition to a polarized domain state is visible. (c)–(e) Trajectory of the susceptibility for different protocols. Numbers indicating the sequence of the field changes. (c) Staying below the critical field  $H^*$  the state is stable. (d,e) The state can be changed by applying a high positive or negative field or thermal cycling. (f) ac susceptibility for different applied fields,  $H^0$ , while cooling the sample below  $T_N$ .

polarized domain walls present within a nonmagnetic bulk background phase. This explains (a) the negative remanence, (b) the tunability of the hysteresis via cooling in a finite field, (c) the resetting of the sample state via a heat pulse, and (d) the anisotropy.

We note the effective nature of the theory presented below. In particular, we cannot account microscopically for how the domain walls are formed dynamically, and which spatial structure ultimately emerges. However, we also stress its success in explaining the experimental phenomenology.

We model the system via a free energy for a mixture of two bulk phases with different energies given by

$$f = x[E_{\text{AIAO}}(H) - E_{\text{AOAI}}(H)] + x(1-x)[E_{\text{DW}} - m_{\text{DW}}H] + T[x \ln(x) + (1-x) \ln(1-x)], \quad (1)$$

with the volume fraction  $x$  of the AIAO bulk phase, the corresponding bulk energies  $E_{\text{AIAO/AOAI}}$ , a contribution of the domain walls proportional to the surface between phases  $x(1-x)$  with associated cost  $E_{\text{DW}}$  due to broken bonds and magnetization  $m_{\text{DW}}$ , and the mixing entropy between phases proportional to the temperature  $T$ .

For the comparison with the experimental hysteresis curves in Figs. 2(a) and 2(b) we use the energy and magnetization of the bulk phases obtained from a classical treatment of the microscopic Hamiltonian which reproduces the magnetization behavior observed for magnetic fields oriented along [001] (see Supplemental Material). We emphasize that we do not fit parameters to the hysteretic data, but rather use the parameters obtained from the nonhysteretic magnetization

curve observed for a different field direction and obtain good agreement with the hysteretic experimental data.

This model is based on the following key observations: The two realizations of the all-in–all-out order, degenerate in energy and carrying no magnetization at zero field, can be split in a magnetic field due to the dipolar–octupolar nature of the  $\text{Nd}^{3+}$  ions [25]. Thus, we model the system as a mixture of two bulk phases with an energy difference dependent on the applied magnetic field.

In particular, the states split for a field applied oriented along  $H \parallel [111]$ , whereas for  $H$  parallel to [001], the field does not distinguish between the AIAO/AOAI states. This explains the observed anisotropy of the hysteresis, present for  $H \parallel [111]$ , and absent for  $H \parallel [001]$ .

To explain the negative remanence we note that domain walls carry a magnetization  $m_{\text{DW}}$ , and suggest that this magnetization preferentially opposes the applied field. We argue that domain walls between AIAO and AOAI domains with a negative magnetization are kinematically favored as they have a lower-energy barrier than walls with a positive magnetization (see Supplemental Material).

In consequence, once domains have formed at low temperature and finite field, the sample retains a negative remanent magnetization after removing the field: In zero field, both AIAO and AOAI domains have zero magnetization, so that only that of the domain walls remains.

Naturally, the magnetization of a random collection of domain walls vanishes. Thus, applying a heat pulse  $T > T_N$  to the sample allows a relaxation of the domains in which all symmetry equivalent domains are created equally, resulting in a vanishing magnetization.

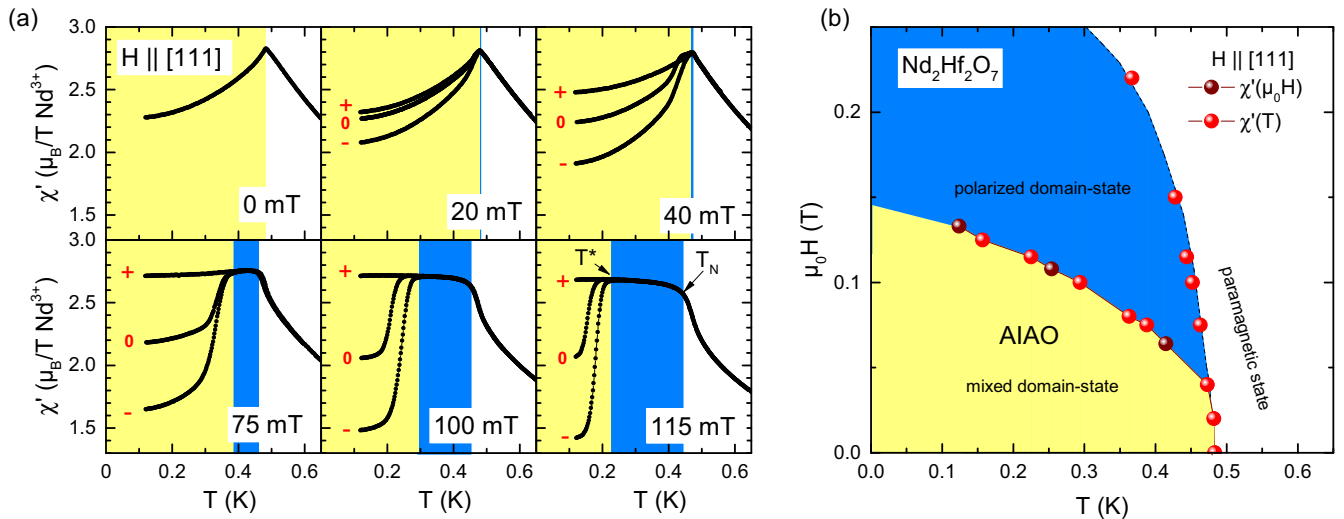


FIG. 3. (a) Temperature dependence of the dynamic susceptibility of  $\text{Nd}_2\text{Hf}_2\text{O}_7$  for magnetic dc fields applied along  $H \parallel [111]$ . The sample was prepared to be either in the positive polarized state (+), the negative polarized state (−), or the unpolarized state (0). The blue shaded area denotes the respective temperature range of the single-domain state. (b) Phase diagram for  $\text{Nd}_2\text{Hf}_2\text{O}_7$  for  $H \parallel [111]$ . The phase boundary of the all-in-all-out order was determined by the kinks/peaks of  $\chi'(T)$  (red spheres). The border between the mixed domain phase and the polarized domain phase was constructed by taking the temperature at each field (red spheres) below which the ac susceptibility starts to differ when polarizing in negative compared to positive external fields  $|H| > H_c$  and the field strength of the end points of the hysteresis in the dynamic susceptibility (brown spheres). The thin black dashed line is a guide to the eye.

When preparing the sample in a partially polarized state by cooling down in a finite field, both AIAO and AAOI domains are present with a ratio determined by the field-strength-induced splitting of the states and tunable from fully positive to fully negatively polarized. The hysteresis curve then follows the weighted average of the fully positively and fully negatively polarized sample states.

Our findings constitute the observation of an inverted hysteresis/negative remanence in a bulk antiferromagnet. The proposed mechanism—a nonequilibrium population of negatively polarized domain walls—invites more detailed investigations, in particular, with regard to the nucleation process leading to the disappearance of the phenomenon, and the spatial distribution of the domain walls themselves.

By contrast, previous instances of negative remanence were essentially ferrimagnetic in nature, in that they relied on the noncancellation of moments of inequivalent ferromagnetic subsystems, either in the form of thin films [27,29,30] or different ionic species [31–33].

Not only is our hysteresis loop highly reproducible and robust to magnetic field and temperature changes, but also

exquisitely tunable. We demonstrate precise control of the system’s response and the preparation of a continuous family of distinct nonequilibrium states.

Thus,  $\text{Nd}_2\text{Hf}_2\text{O}_7$  provides a nonequilibrium landscape controllable via small magnetic fields or temperature pulses. Controlled tunability of magnetic structures underpins the field of spintronics [34–37], and currently the search for novel types of magnetic structures and their manipulation is a central theme there. The preferential coupling in  $\text{Nd}_2\text{Hf}_2\text{O}_7$  of a weak field to domain walls provides an unusual handle on this unconventional magnet, while the antiferromagnetic domains themselves do not interact with each other via a bulk magnetization. Each of these items is desirable for technological applications underlining the potential for inclusion in submicron devices.

We acknowledge the Helmholtz-Gemeinschaft for funding via the Helmholtz Virtual Institute (Project No. VH-VI-521) and Deutsche Forschungsgemeinschaft (DFG) through SFB 1143. We also acknowledge support by HLD at HZDR, member of the European Magnetic Field Laboratory (EMFL).

- [1] X. Wan, A. M. Turner, A. Vishwanath, and S. Y. Savrasov, *Phys. Rev. B* **83**, 205101 (2011).
- [2] J. E. Moore, *Nature (London)* **464**, 194 (2010).
- [3] L. Balents, *Nature (London)* **464**, 199 (2010).
- [4] X.-L. Qi, T. L. Hughes, and S.-C. Zhang, *Phys. Rev. B* **78**, 195424 (2008).
- [5] J. S. Gardner, M. J. P. Gingras, and J. E. Greedan, *Rev. Mod. Phys.* **82**, 53 (2010).
- [6] T.-H. Arima, *J. Phys. Soc. Jpn.* **82**, 013705 (2012).

- [7] S. Tardif, S. Takeshita, H. Ohsumi, J.-i. Yamaura, D. Okuyama, Z. Hiroi, M. Takata, and T.-H. Arima, *Phys. Rev. Lett.* **114**, 147205 (2015).
- [8] T. C. Fujita, Y. Kozuka, M. Uchida, A. Tsukazaki, T. Arima, and M. Kawasaki, *Sci. Rep.* **5**, 9711 (2015).
- [9] E. Y. Ma, Y.-T. Cui, K. Ueda, S. Tang, K. Chen, N. Tamura, P. M. Wu, J. Fujioka, Y. Tokura, and Z.-X. Shen, *Science* **350**, 538 (2015).

- [10] T. C. Fujita, M. Uchida, Y. Kozuka, S. Ogawa, A. Tsukazaki, T. Arima, and M. Kawasaki, *Appl. Phys. Lett.* **108**, 022402 (2016).
- [11] Y. Kozuka, T. C. Fujita, M. Uchida, T. Nojima, A. Tsukazaki, J. Matsuno, T. Arima, and M. Kawasaki, *Phys. Rev. B* **96**, 224417 (2017).
- [12] S. M. Disseler, *Phys. Rev. B* **89**, 140413 (2014).
- [13] Z. Tian, Y. Kohama, T. Tomita, H. Ishizuka, T. H. Hsieh, J. J. Ishikawa, K. Kindo, L. Balents, and S. Nakatsuji, *Nat. Phys.* **12**, 134 (2016).
- [14] C. Donnerer, M. C. Rahn, M. M. Sala, J. G. Vale, D. Pincini, J. Stempffer, M. Krisch, D. Prabhakaran, A. T. Boothroyd, and D. F. McMorrow, *Phys. Rev. Lett.* **117**, 037201 (2016).
- [15] J. J. Ishikawa, E. C. T. O'Farrell, and S. Nakatsuji, *Phys. Rev. B* **85**, 245109 (2012).
- [16] H. Guo, C. Ritter, and A. C. Komarek, *Phys. Rev. B* **96**, 144415 (2017).
- [17] J. Yamaura, K. Ohgushi, H. Ohsumi, T. Hasegawa, I. Yamauchi, K. Sugimoto, S. Takeshita, A. Tokuda, M. Takata, M. Udagawa, M. Takigawa, H. Harima, T. Arima, and Z. Hiroi, *Phys. Rev. Lett.* **108**, 247205 (2012).
- [18] A. Bertin, P. Dalmas de Réotier, B. Fåk, C. Marin, A. Yaouanc, A. Forget, D. Sheptyakov, B. Frick, C. Ritter, A. Amato, C. Baines, and P. J. C. King, *Phys. Rev. B* **92**, 144423 (2015).
- [19] E. Lhotel, S. Petit, S. Guitteny, O. Florea, M. Ciomaga Hatnean, C. Colin, E. Ressouche, M. R. Lees, and G. Balakrishnan, *Phys. Rev. Lett.* **115**, 197202 (2015).
- [20] J. Xu, V. K. Anand, A. K. Bera, M. Frontzek, D. L. Abernathy, N. Casati, K. Siemensmeyer, and B. Lake, *Phys. Rev. B* **92**, 224430 (2015).
- [21] V. K. Anand, A. K. Bera, J. Xu, T. Herrmannsdörfer, C. Ritter, and B. Lake, *Phys. Rev. B* **92**, 184418 (2015).
- [22] T. C. Fujita, M. Uchida, Y. Kozuka, W. Sano, A. Tsukazaki, T. Arima, and M. Kawasaki, *Phys. Rev. B* **93**, 064419 (2016).
- [23] H. T. Hirose, J.-I. Yamaura, and Z. Hiroi, *Sci. Rep.* **7**, 42440 (2017).
- [24] K. Ueda, J. Fujioka, B.-J. Yang, J. Shiogai, A. Tsukazaki, S. Nakamura, S. Awaji, N. Nagaosa, and Y. Tokura, *Phys. Rev. Lett.* **115**, 056402 (2015).
- [25] L. Opherden, J. Hornung, T. Herrmannsdörfer, J. Xu, A. T. M. N. Islam, B. Lake, and J. Wosnitza, *Phys. Rev. B* **95**, 184418 (2017).
- [26] See Supplemental Material at <http://link.aps.org/supplemental/10.1103/PhysRevB.98.180403> for further experimental data and details as well as assumptions made concerning the presented free-energy calculations, which includes Refs. [38–40].
- [27] T. Maity, D. Kepaptsoglou, M. Schmidt, Q. Ramasse, and S. Roy, *Phys. Rev. B* **95**, 100401 (2017).
- [28] Z. M. Tian, Y. Kohama, T. Tomita, J. Ishikawa, H. Mairo, K. Kindo, and S. Nakatsuji, *J. Phys.: Conf. Ser.* **683**, 012024 (2016).
- [29] A. Aharoni, *J. Appl. Phys.* **76**, 6977 (1994).
- [30] K. Takanashi, H. Kurokawa, and H. Fujimori, *Appl. Phys. Lett.* **63**, 1585 (1993).
- [31] S.-I. Ohkoshi, T. Hozumi, and K. Hashimoto, *Phys. Rev. B* **64**, 132404 (2001).
- [32] Y. Z. Wu, G. S. Dong, and X. F. Jin, *Phys. Rev. B* **64**, 214406 (2001).
- [33] J.-M. L. Beaujour, S. N. Gordeev, G. J. Bowden, P. A. J. de Groot, B. D. Rainford, R. C. C. Ward, and M. R. Wells, *Appl. Phys. Lett.* **78**, 964 (2001).
- [34] V. Baltz, A. Manchon, M. Tsoi, T. Moriyama, T. Ono, and Y. Tserkovnyak, *Rev. Mod. Phys.* **90**, 015005 (2018).
- [35] S. Bader and S. Parkin, *Annu. Rev. Condens. Matter Phys.* **1**, 71 (2010).
- [36] I. Žutić, J. Fabian, and S. Das Sarma, *Rev. Mod. Phys.* **76**, 323 (2004).
- [37] D. A. Allwood, G. Xiong, C. C. Faulkner, D. Atkinson, D. Petit, and R. P. Cowburn, *Science* **309**, 1688 (2005).
- [38] Y.-P. Huang, G. Chen, and M. Hermele, *Phys. Rev. Lett.* **112**, 167203 (2014).
- [39] O. Benton, *Phys. Rev. B* **94**, 104430 (2016).
- [40] S. Petit, E. Lhotel, B. Canals, M. Ciomaga Hatnean, J. Ollivier, H. Mutka, E. Ressouche, A. R. Wildes, M. R. Lees, and G. Balakrishnan, *Nat. Phys.* **12**, 746 (2016).